THE ANNALS OF "DUNAREA DE JOS" UNIVERSITY OF GALATI.
FASCICLE IX. METALLURGY AND MATERIALS SCIENCE
N^0. 2 – 2007, ISSN 1453 – 083X

STUDY OF THE THERMODYNAMIC REGIME AT THE CONTINUOUS CASTING OF STEEL

Alexandru IVANESCU, Lilica IVANESCU, Ciresica Cocindau, Viorel MUNTEANU
"Dunarea de Jos" University of Galati
e-mail: ivanescu1944@yahoo.ca;

ABSTRACT

The paper presents the evolution of the heat exchange coefficient along the path of the continuous casting unit, as a function of the cooling water flow rate and the path length. The optimization of this thermodynamic regime assures the improvement of the quality of the continuous cast slabs and the increasing of the rate of obtaining the qualitatively corresponding slabs.

KEYWORDS: continuous casting, heat transfer

1. Introduction

- The secondary cooling in a continuous casting unit (**Figure 1**) represents the part of the machine in which the solidification, started in the crystallizer, ends.

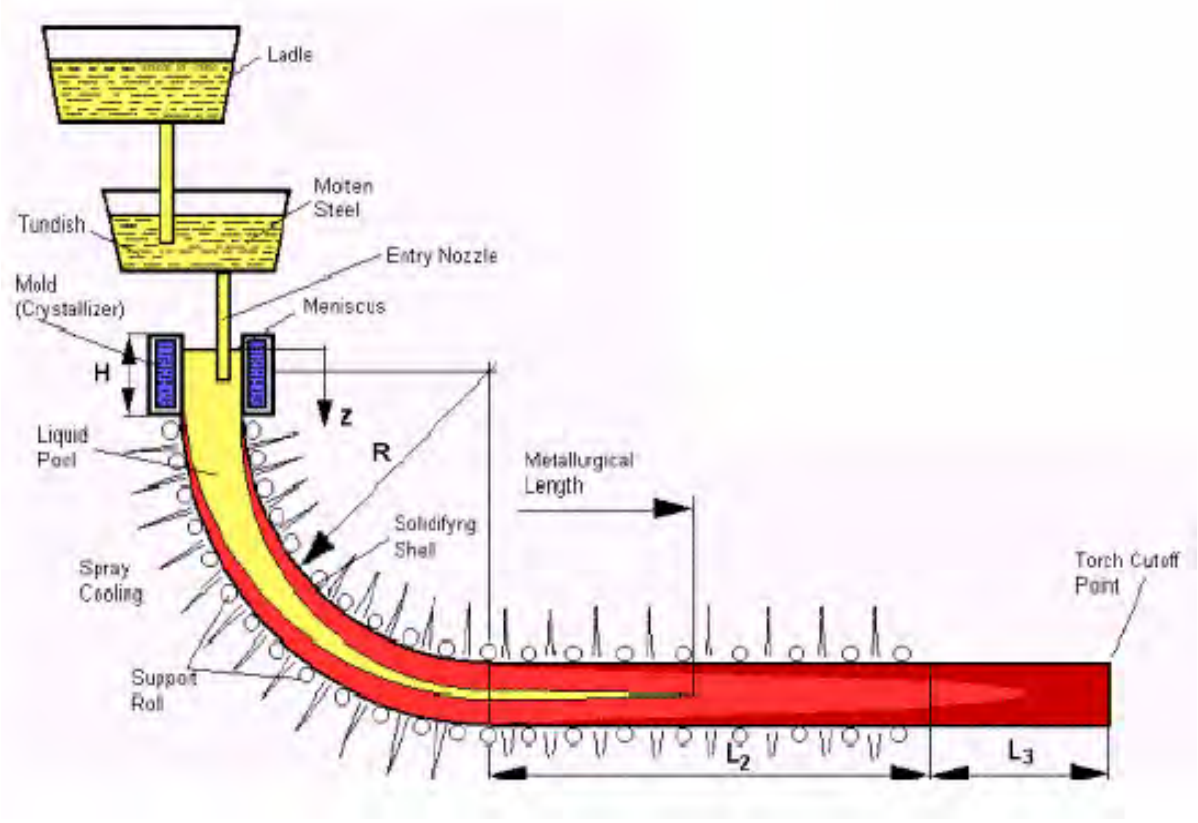

Fig. 1. *Scheme of a continuous caster*

In this zone there can be distinguished different elementary mechanisms of transfer which contribute to the evacuation of the heat from the slab surface:

- the radiation of the slab surface toward the environment;
- the convection of the environmental air, whose importance is smaller than the other heat transfer ways;
- the conduction at the direct contact of the slab surface with the rolls;
- the direct transfer to the pulverized water, the impact of the water droplets with the warm slab surface;
- the transfer by superficial boiling of water, which splashes along the surface or is accumulated by the supporting rolls. The heat repartition among these transfer ways depends on the machine type and the regulating conditions of the splashing and the approximated percentages of the evacuated heat in different ways are:
- radiation ……..……..……28 %
- air convection……...….0.5 %
- conductibility in rolls ……17 %
- direct transfer at the rolls impact..16 %
- transfer at the cooling water……38.5 %

The thickness of the solidified crust increases in the secondary cooling region as the removed heat quantity increases. The rate of the crust thickness increasing, is proportional to the removed heat quantity, which size depends on the heat exchange coefficient, α.

2. Experimental researches

The heat exchange coefficient, α, was determined using the relation [1-4]:

$$\alpha = Nu \cdot \frac{\lambda}{\ell} \ [\text{W/m}^2\text{K}], \qquad (1)$$

where: λ is the thermal conductibility of the fluid, in [W/m.K]; ℓ - the determinative length of the heat exchange (the dimension along the direction of the fluid flow), in [m]; Nu – the Nusselt criterion,

$$Nu = 0.151 \cdot Re^{0.8} \cdot Pr^{0.75} \qquad (2) \ ;$$

$$Re = \frac{w\,d}{\upsilon} \qquad (3) \ ;$$

$$w = \frac{D_a}{A_d} \qquad (4) \ ,$$

with Re – Reynolds' criterion, Pr – Prandtl criterion, w – is the cooling water rate of flow, in [m/s]; d – the nozzle diameter, in [m]; υ – the cinematic viscosity, in [m^2/s]; D_a - the cooling water flow rate, in [m^3/s]; A_d - the nozzle area, in [m^2]. In order to calculate the heat exchange coefficient the following characteristics of the cooling water have been used:

- the temperature ……15 ^{o}C ÷ 100 ^{o}C
- the thermal conductibility λ [W/m.K] ……..0.588 ÷ 0.682
- the cinematic viscosity υ [m^2/s] ……0.136 ·10^{-6} ÷ 0.29 ·10^{-6}
- Prandtl criterion 8.689 ÷ 1.716.

Table 1

Impact density [l/m^{2}min]	α [W/m^{2}K]	α [W/m^{2}K]
75	419.3	409.76
150	555.4	558.23
300	834.3	845.44
450	1108.6	1119.66
600	1398.3	1380.90
750	1626.3	1629.17
900	1872.6	1864.45
1050	2079.4	2086.75

3. Data processing

In Table 1 are presented the impact densities of the cooling water jets and the corresponding heat exchange coefficients.

From Figure 2 it can be seen that the heat exchange coefficient increases linearly with the increasing of the impact density.

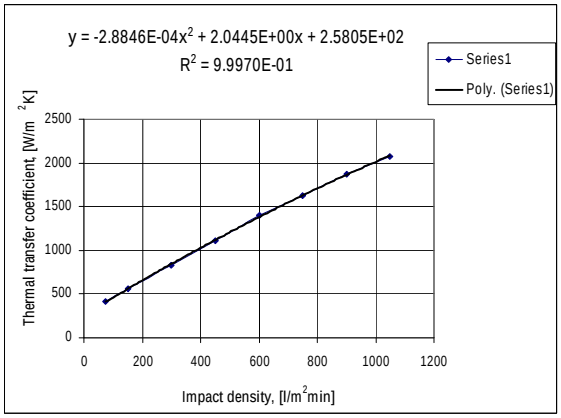

***Fig. 2** The thermal transfer coefficient*

Were determinate the steel temperatures in the distributor, the cooling water temperatures of the crystallizer at the entrance and at the exit, the temperatures of the crystallizer plates on the fixed part and on the mobile part. The data processing is presented in Figure 3.

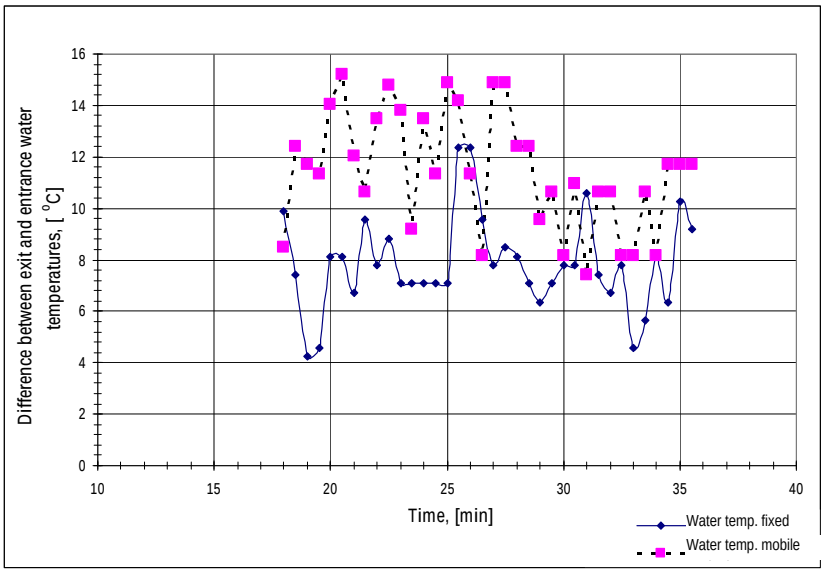

***Fig. 3** Cooling water temperatures*

In Table 3 are presented the secondary cooling zones with the nozzles types which run in these zones, the lengths of the zones, the splashing angles of the nozzles, their diameters and the technological flow rates on the nozzles, as well, for a pressure of 1 atm and 3 atm.

Table 3

Nozzle position	Nozzle type	Zone length	Splashing angle	Dimensions	Equivalent diameter, d	Nozzle area, A_d	Distance, h	Flow length, l	Number of nozzles	Technological flow rate per nozzle, D		Technological flow rate per nozzle, D	
										1 atm	3 atm	1 atm	3 atm
		[m]	[°]	[mm]	[mm]	[mm^2]	[m]	[m]	[no.]	[l/min]		[m^3/h]	
Zone Ia fixed	**7680F**	**0.70**	120	1.6*10.77	3.38	17.23	0.115	0.398	8	6.66	11.53	0.400	0.692
	6065L		90	2.4	2.4	4.52	0.080	0.160	30	4.73	8.19	0.284	0.492
Zone Ia mobile	**7680F**	**0.69**	120	1.6*10.77	3.38	17.23	0.115	0.398	8	6.66	11.53	0.400	0.692
	6065L		90	2.4	2.4	4.52	0.080	0.160	30	4.73	8.19	0.284	0.492
Zone Ib fixed	**5580F**	**0.90**	120	1.3*11.29	3.12	14.68	0.110	0.381	25	6.15	10.64	0.369	0.639
Zone Ib mobile	**5580F**	**0.88**	120	1.3*11.29	3.12	14.68	0.110	0.381	25	6.15	10.64	0.369	0.639
Lateral left	**7680F**	**1.60**	120	1.6*10.77	3.38	17.23	0.080	0.277	2	6.66	11.53	0.400	0.692
	3565L		90	1.9	1.9	2.83	0.110	0.220	11	3.75	6.49	0.225	0.389
Lateral right	**7680F**	**1.57**	120	1.6*10.77	3.38	17.23	0.080	0.277	2	6.66	11.53	0.400	0.692
	3565L		90	1.9	1.9	2.83	0.110	0.220	11	3.75	6.49	0.225	0.389
Zone II fixed	**C200100**	**2.90**	120	1.3*27.5	4.87	35.75	0.395	1.368	10	9.59	16.61	0.576	0.997
Zone II mobile	**C200100**	**2.88**	120	1.3*27.5	4.87	35.75	0.395	1.368	10	9.59	16.61	0.576	0.997
Zone III fixed	**C120100**	**3.00**	120	1*27.5	4.27	27.50	0.395	1.368	8	8.41	14.57	0.505	0.874
Zone III mobile	**C110100**	**2.89**	120	1*27.5	4.27	27.50	0.395	1.368	8	8.41	14.57	0.505	0.874
Zone IV fixed	**664847**	**4.40**	120	1.45*20.94	4.48	30.36	0.425	1.472	12	8.84	15.31	0.530	0.919
Zone IV mobile	**664677**	**4.34**	120	1.05*20.94	3.82	21.99	0.425	1.472	12	7.52	13.03	0.451	0.782

On the basis of these data, using the relations 1÷4, there have been calculated the cooling water rates of flow, the *Re* and *Nu* criteria, and the heat exchange coefficient, α, at the cooling water pressure of 1 atm and 3 atm, respectively, which are presented in Table 4.

Table 4

Nozzle position	Nozzle type	*Re*	*Nu*	Rate of flow, *w*			
				1 atm	3 atm	1 atm	3 atm
				[m/s]		[W/m^{2}K]	
Zone Ia fixed	**7680F**	19157	33177	6.44	11.16	3007	4666
	6065L	36840	63802	17.44	30.20	12633	19603
Zone Ia mobile	**7680F**	19157	33177	6.44	11.16	3007	4666
	6065L	36840	63802	17.44	30.20	12633	19603
Zone Ib fixed	**5580F**	19157	33177	6.98	12.09	3144	4878
Zone Ib mobile	**5580F**	19157	33177	6.98	12.09	3144	4878
Lateral left	**7680F**	19157	33177	6.44	11.16	4323	6708
	3565L	36840	63802	22.03	38.15	9188	14257
Lateral right	**7680F**	19157	33177	6.44	11.16	4323	6708
	3565L	36840	63802	22.03	38.15	9188	14257
Zone II fixed	**C200100**	19157	33177	4.47	7.74	875	1359
Zone II mobile	**C200100**	19157	33177	4.47	7.74	875	1359
Zone III fixed	**C120100**	19157	33177	5.10	8.83	875	1359
Zone III mobile	**C110100**	19157	33177	5.10	8.83	875	1359
Zone IV fixed	**664847**	19157	33177	4.85	8.40	814	1263
Zone IV mobile	**664677**	19157	33177	5.70	9.88	814	1263

With the aid of the values presented in Table 3 and those calculated in Table 4, the following dependences have been represented: the variation of the cooling water flow rate along the path length on the fixed part, at the cooling water pressures of 1 atm and 3 atm (Figure 4); the variation of the heat exchange coefficient along the path length on the fixed part, at the cooling water pressures of 1 atm and 3 atm (Figure 5); the variation of the cooling water flow rate along the path length on the mobile part, at the cooling water pressures of 1 atm and 3 atm (Figure 6); the variation of the heat exchange coefficient along the path length on the mobile part, at the cooling water pressures of 1 atm and 3 atm (Figure 7).

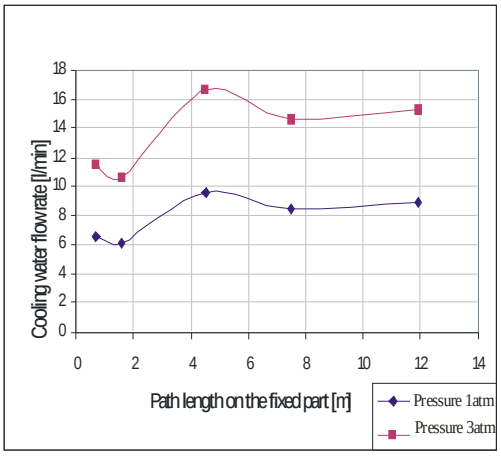

Fig.4. *Variation of the cooling water flow rate along the curved path (fixed part).*

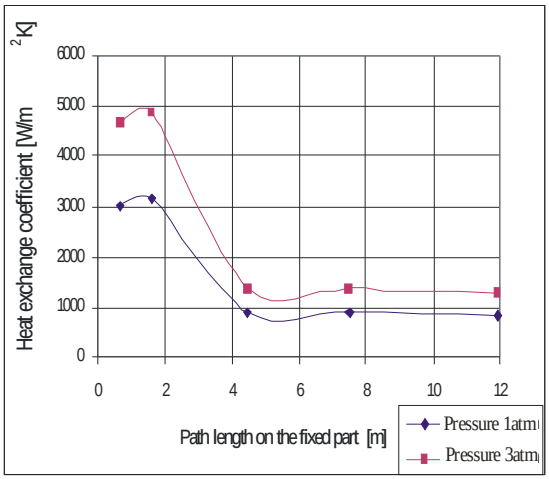

Fig.5. *Variation of the heat exchange coefficient along the curved path (fixed part)*

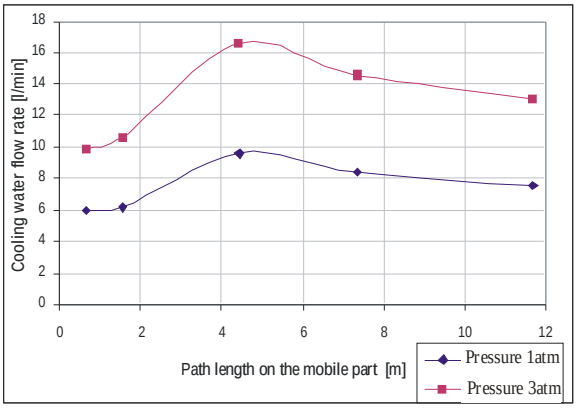

Fig.6. *Variation of the cooling water flow rate along the curved path (mobile part)*

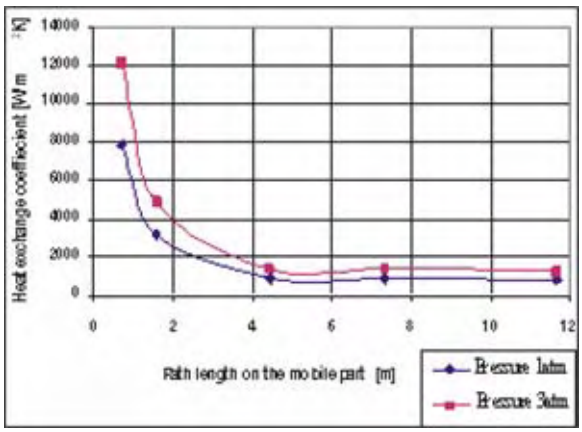

Fig.7. *Variation of the heat exchange coefficient along the curved path (mobile part).*

4. Conclusions

The heat exchange coefficient increases linearly with the increasing of the impact density of the cooling water jets. The difference between the cooling water temperature of the crystallizer at the exit and the temperature at the entrance is bigger at the cast beginning and is reducing as the cast duration increases. The variations of the cooling water flow rates along the path, both on the fixed part and on the mobile part, have similar curve rates, presenting a maximum at approximately 4 m from the crystallizer exit. On the mobile part, this maximum flow rate is achieved for a bigger value, as compared with the fixed part of the unit. The coefficient of heat exchange presents a minimum corresponding to the maximum in the diagram of cooling water flow rate, at approximately 4 m from the crystallizer exit. On the mobile part, the coefficient of heat exchange has bigger values than on the fixed part.

References

[1].Stefanescu, D., Leca, A., Luca, L., Badea, A., Marinescu, M., *Heat and mass transfer. Theory and applications,* Bucharest: Editura Didactica si Pedagogica, 1983.
[2].Ivanescu, A., *Mass transfer at the metallic materials processing*, Bucharest: Editura Didactica si Pedagogica, 2004.
[3].Dragomir, I. *Theory of the iron and steel processes*, Bucharest: Editura Didactica si Pedagogica, 1985.
[4].Munteanu, V., Geanta, M., *Casting of semi-products,* Bucharest: Editura Universitatii Politehnica, 2005.